Measurement of atomic Stark parameters of many MnI and FeI spectral lines using GMAW process

S Zielinska, S Pellerin, K Dzierzega, Flavien Valensi, K Musiol, F Briand

Measurement of atomic Stark parameters of many Mn I and Fe I spectral lines using GMAW process

S Zielinska[1,2], S Pellerin[1#], K Dzierzega[2], F Valensi[1,3], K Musiol[2] and F Briand[4]

[1] *GREMI, Université d'Orléans (Site de Bourges) / CNRS, BP 4043, 18028 Bourges cedex, France*
[2] *Marian Smoluchowski Institute of Physics, Jagellonian University, Krakow, Poland*
[3] *LAPLACE-AEPPT, Université Paul Sabatier/CNRS, 31062 Toulouse cedex 9, France*
[4] *CNRS, UPR3079 CEMHTI, 1D av. de la Recherche Scientifique, 45071 Orléans cedex 2, France*

E-mail adresses : sylwia.zielinska@airliquide.com
stephane.pellerin@univ-orleans.fr
krzycho@netmail.if.uj.edu.pl
flavien.valensi@laplace.univ-tsle.fr
ufmusiol@cyf-kr.edu.pl
francis.briand@airliquide.com

Abstract: The particular character of the welding arc working in pure argon, which emission spectrum consists of many spectral lines strongly broadened by Stark effect, has allowed to measure, sometimes for the first time, the Stark parameters of 15 Mn I and 10 Fe I atomic spectral lines, and to determine the dependence in temperature of normalized Stark broadening in $N_e = 10^{23}$ m^{-3} of the 542.4 nm atomic iron line. These results show that special properties of the MIG plasma may be useful in this domain because composition of the wire-electrode may be easily adapted to needs of an experiment.

Keywords: GMAW, Stark parameters, optical emission spectroscopy, diagnostic, Mn, Fe

PAC number : 52.25.Os, 52.50.Dg, 52.50.Nr, 52.70.Kz, 52.75.Hn, 52.77.Fv

Submitted to : *Journal of Physics D: Applied Physics*
for the 'Metal vapour' **cluster issue**

Author to whom correspondance should be adressed : stephane.pellerin@univ-orleans.fr

1. Introduction

The knowledge of absolute value for Stark parameters is crucial in many fields of science and technology. For instance, Stark parameters and oscillator strengths are indispensable in simulations of radiation transport in dense plasma in laboratory and of astrophysical origin. Another class of applications is related to direct dependence of Stark broadening on electron and ion concentrations. This dependence enables determination of electron density N_e by measuring emission or absorption profiles of the spectral lines. Such diagnostic method can be applied only when Stark broadening was either theoretically calculated or determined in independent experiment where N_e was determined by another method. In this frame, since 1976, the NBS/NIST (U.S.A.) has published a few compilations of experimental Stark broadening parameter appearing in the literature [1-5], estimating the accuracy of published data.

Researches on the emission spectrum of metallic elements, and in particular on the determination of Stark broadening and displacement of spectral lines, are very difficult because of the need to introduce the atoms to be analyzed in the middle of the discharge zone. In general, in the case of the plasmas used in laboratory, that is not simple and induces important problems of demixing effect that are difficult to solve. This difficulty mainly explains the absence of experimental data available in the literature. And yet the knowledge of the Stark parameters of atom and ionic spectral lines is of considerable importance, either for the diagnosis of laboratory plasmas or for the knowledge of the plasma-producing mediums studied in astrophysics.

In the gas metal arc welding (GMAW) processes, an arc discharge between a consumable solid metal electrode and a weld pool is used. The wire-electrode, liquid metal transferring inside arc and weld pool are protected against air by a shielding gas flux: an inert gas in the case of the MIG (Metal Inert Gas) welding or a chemically active one in the case of the MAG (Metal Active Gas) process. These welding methods are used in all sectors of activity to assemble all grades of metal (ferrous and non-ferrous). The schematic description of the welding torch is presented in Figure 1.

The MIG type discharge was not considered until now as a plasma source which could be applied to the measurement of the Stark parameters of spectral lines. That is hardly astonishing, if one takes into account the actual lack of knowledge concerning the phenomena which occur in this type of plasma, the questions of the validity of the local thermodynamical equilibrium in such plasmas (that is generally required to use the classical optical emission spectroscopy methods to diagnose the medium – See discussions in different papers of this issue, for example by F.Valensi *et al* [6]) and more particularly, the absence of experimental data relating to the distributions of electronic temperatures T_e and density N_e in the plasma-producing medium. These two parameters strongly depend on the nature of shielding gas and chemical composition of the electrodes used.

Recent experimental results concerning the diagnosis of MIG welding plasmas without assumption on the equilibrium state of the plasma-producing medium [6-9], allow considering this type of plasma like sources of atomic metrology particularly interesting for the study of the metal lines of chosen elements.

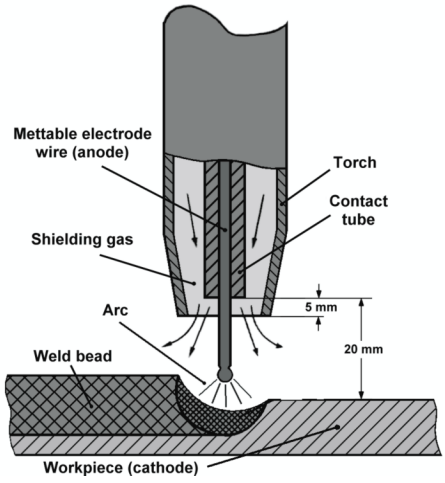

Figure 1 - MIG/MAG welding torch diagram.
Anode - the wire with feed rate of v_{wire} =9 m.min^{-1}. Cathode - the mild steel metal plate. The shielding gas – pure Ar.

2. Conditions of measurement

The experimental system is presented in [7, 8, 9]. Here we present only most important points (See Figures 1 and 2). The plasma was generated by a welding set SAFMIG 480 TRS PLUS equipped with a SAFMIG 480 TR 16 kit. The wire-anode used in our experiments was a mild steel consumable electrode (AWS A5.17 – See composition in Table 1) with a diameter of 1.2 mm. The workpiece, that plays the role of cathode, is a mild steel metal plate (EN 10025 S235 JRG2) with section of 30×8 mm and 300 mm length : its composition is given in table 1.

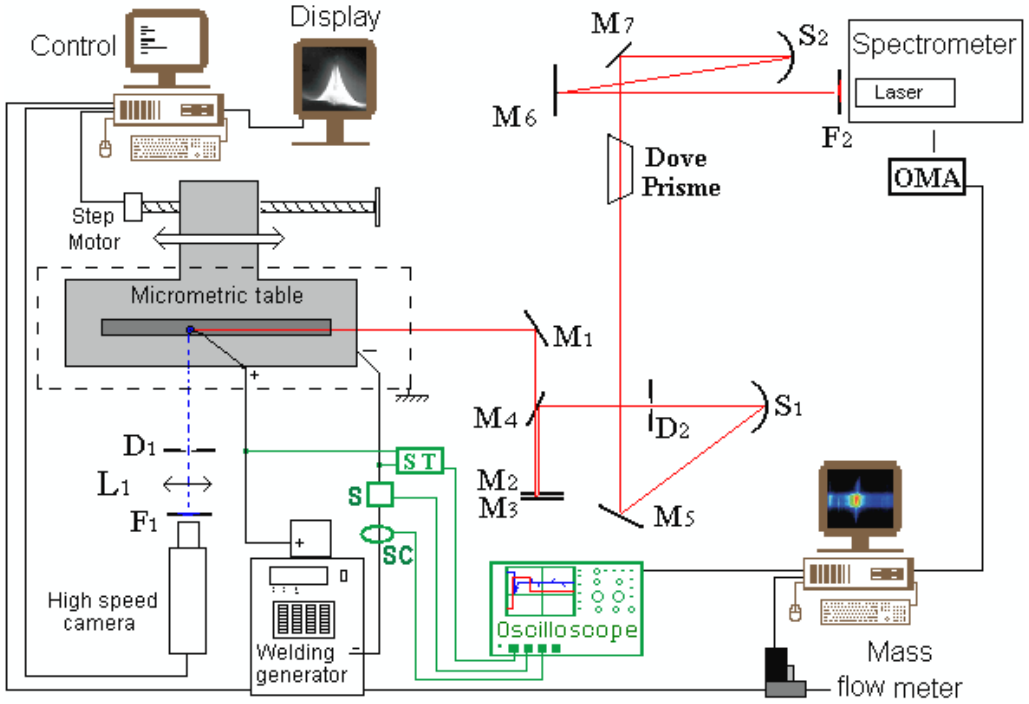

Figure 2. Experimental set-up.
F_1, F_2 – optical filters; M_1..M_7 - flat mirrors; S_1,S_2 - spherical mirrors; D_1,D_2 - diaphragms; L_1 - lens; DP - Dove's prism; ST - voltage probe; SC- current probe; S – shunt.

Element	wt.%	at.%
Fe	98.17	97.46
Mn	1.070	1.080
Si	0.350	0.691
Cu	0.160	0.140
C	0.087	0.402
Ni	0.058	0.055
Mo	0.038	0.022
Cr	0.022	0.023
O	0.014	0.049
P	0.011	0.020
S	0.011	0.019
Co	0.008	0.008
N	0.006	0.025
V	0.002	0.002
Nb	0.002	0.001
Ti	0.001	0.001
Al	< 0.001	< 0.002
Zr	< 0.001	< 0.001
B	0.0002	0.001

a/ Anode wire

Element	wt.%	at.%
Fe	98.30	97.97
Mn	0.490	0.496
Si	0.140	0.277
C	0.059	0.273
P	0.037	0.066
S	0.046	0.080
Cr	0.145	0.155
Mo	0.031	0.018
Ni	0.158	0.150
Al	0.003	0.006
Co	0.014	0.013
Cu	0.519	0.455
Nb	0.002	0.001
Ti	0.002	0.002
V	0.001	0.001
W	0.005	0.002
Sn	0.021	0.010
As	0.020	0.015
Zr	0.001	0.001
Ca	0.0005	0.0007
Se	0.0019	0.0013
B	0.0002	0.0010

b/ Cathode plate

Table 1. Composition of the electrodes

During the welding, a micrometric table driven by step motor ensured the displacement of the workpiece (cathode) with horizontal velocity 4 mm.s^{-1}. The measurements of voltage U_{arc} between the electrodes and arc current I_{arc} were carried out by a differential voltage probe and current probe (Hall effect transducer). These characteristics of discharge were stored by a numerical oscilloscope.

The power supply worked in the constant current mode, with the same parameters for all measurements. Measurements were performed for pure argon as shielding gas with a flow of 20 L.mn^{-1}, and the average current was set at $I_{average}$ = 326 A. The average value of the voltage $U_{average}$ was close to 36.0 V. In these conditions, the wire speed was fixed to v_{wire} = 9 m.mn^{-1}. Pictures of the plasma were taken by the fast camera. For all experiments measured averages values of the current was stable within 0.5% and the voltage value changes were smaller than 1%.

The observation of the shape oh the plasma and the recordings of the pictures' sequences, were performed with fast camera equipped with photodiodes matrix (see Figure 3). A narrow bandwidth (3 nm full width at half maximum) interferential filter centered at 468.8 nm in front of the camera's objective was used to limit the light intensity and spectral bandwidth in order to get an indication on the metal vapours repartition [10]. In this wavelength window, only metal lines can be observed, such as iron or manganese, and the argon continuum can be considered as proportional to the square electron density. The pictures obtained can then give information not only on the plasma components reparation but also on the current flow geometry.

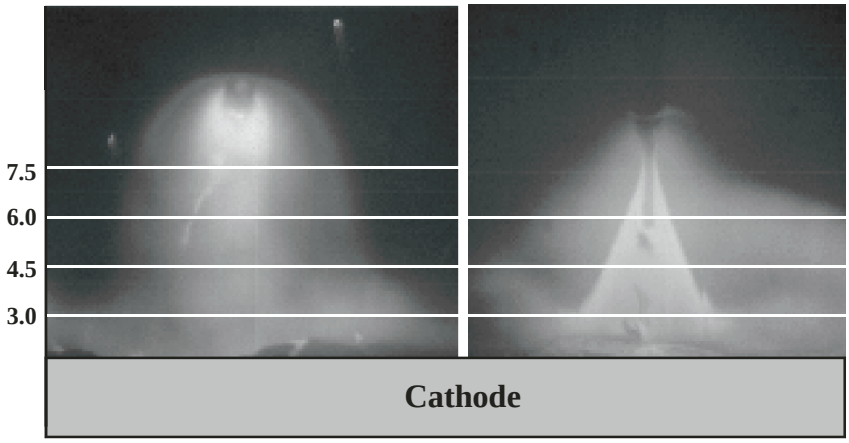

a/ Ar + 20.2%$_{vol}$ CO_2 b/ Pure Argon

Figure 3 - Localization of layers observed in the plasma column. Distances are in mm.

For spectroscopic measurements we used an Ebert type grating spectrometer, with a resolution equal to R = 150000 and reciprocal dispersion of about 0.2 nm.mm^{-1}, equipped with an intensified two-dimensional CCD array of 512×512 contiguous photodiodes (effective size: 24×24 μm), which recorded about 4 nm range of the spectrum. During each experiment about 15 pictures of selected spectrum was recorded, with the CCD exposure time from 50 to 300 ms and delays about 260 ms between consecutive expositions. Configuration of the spectrometer causes a tilt of spectral lines on the CCD picture (figure 4). It was numerically corrected before data were used for calculation.

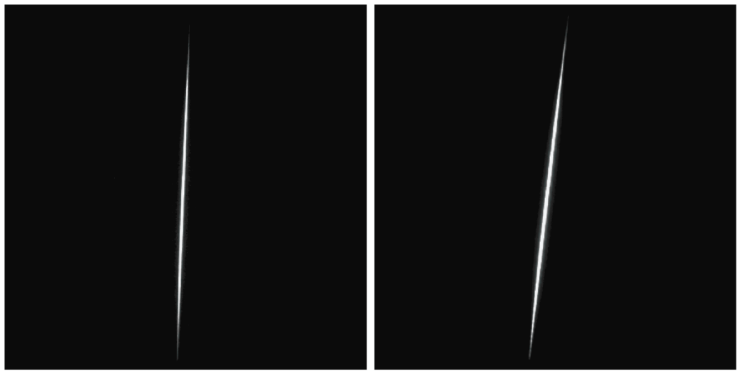

a/ 430.0 nm Ar I (-2.4°) b/ 696.5 nm Ar I (-6.9°)

Figure 4 – Tilt of spectral lines on CCD picture

Optical system with the Dove's prism turned the image of the discharge at the entrance slit of the spectrometer by 90^0. The width of the entrance slit of the spectrometer was set to 20 μm, corresponding to its normal value for wavelength of 400 nm. Spectroscopic measurements were perform for a plasma layer at the distance h = 4.5 mm from the cathode.

An independent experiment consisted of the following sequence: selection of experimental parameters - plasma was switched on for about fifteen seconds – all data were recorded for stable conditions of discharge – plasma was switched off.

In the chosen working conditions, a stable axial spray transfer mode ("spray-arc") of the melted metal from wire electrode is observed [6-9]: the droplets have a diameter smaller than the wire's, and their frequency of detachment is about 100 Hz (see Figure 3b). One difficulty with this type of plasma is the possible transfer in the arc column while recording, of a drop of melted metal that hides the plasma radiation. But such case is still clearly visible: it results in a dark area in the center of the recordings, both lines of iron lines of argon. Then, the corresponding record is rejected and repeated.

For different experiments, we observed large changes of the light intensity. It was caused by fumes produced by the discharge. Nevertheless, for given experimental conditions, intensity ratios and lines profiles (widths and positions) for different spectral lines were well reproducible (see [7, 8, 9]).

For further processing the most suitable data were selected, with the best axial symmetry and without clear evidence of melted metal drop passage.

In order to determine the most suitable spectral lines for our measurements we registered the emission spectrum of the MAG plasma with Ar + 2.3%$_{vol}$ of CO_2, at the distance of h = 4.5 mm from the cathode (Figure 5). Observed spectral lines were identified with help of tables published by NIST [11] and by compared with the spectrum of iron published by Allen [12].

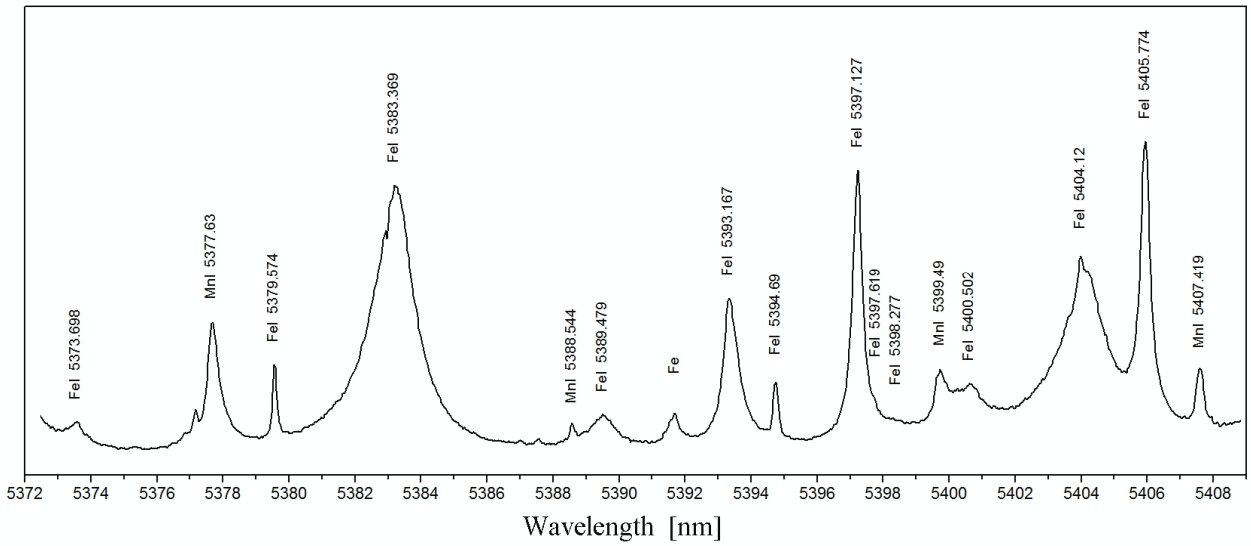

Figure 5 – A part of the spectrum
Experimental conditions: Ar + 2.3%$_{vol}$ CO_2; $I_{arc} \approx$ 330 A; $U_{arc} \approx$ 32 V; v_{wire} = 9 m/mn
Observation of the arc axis at $h \approx$ 4.5 mm from the cathode

3. Data treatment

3.1. Broadening of the spectral line.

Several factors determining broadening of a spectra line one may group into two categories, giving lorentzian and gaussian contribution to the line shape. Apart broadening mechanisms existing in a plasma, the observed line profile is also broadened by the applied spectroscopic device. So called apparatus function is convoluted to the line profile and enlarges the measured one. Deconvolution of apparatus function from measured line is relatively easy to do if the function is known. In our case, for the apparatus function determination, the low-pressure spectral lamps were applied, and the full-width at half-maximum of

apparatus function for the 696.543 nm Ar I line equals to $(0.72\pm0.02)\times10^{-2}$ nm and for the 538.33 nm Fe I line equals to $(0.94\pm0.02)\times10^{-2}$ nm.

In the case of Fe and Ar spectral lines emitted from the MIG-MAG plasmas one may systemize these factors in a following order:

$$\Delta\lambda_N < \Delta\lambda_{vdW} < \Delta\lambda_D \approx \Delta\lambda_A < \Delta\lambda_S \quad (1)$$

Symbols denote full line width at half maximum of: natural, van der Waals, Doppler, apparatus and Stark profile, respectively.

The natural width $\Delta\lambda_N$ of a line is related to the lifetime of the levels connected by the transition and only the ground level of the atom remains quasi-infinitely narrow, as its lifetime is quasi-infinite. In the theory proposed by Wigner and Weisskopf, the natural profile is a lorentzian. In the case of iron, the lifetimes of the upper and lower levels of the transition at 538.4 nm are respectively 12.8 ns and 11.6 ns [13], and the natural width of the iron line is then around 2.5×10^{-5} nm, while that for the 696.5 nm argon line is 9.5×10^{-5} nm [14]: they are negligible in comparison with the widths measured experimentally for arc plasma sources.

Pressure broadening results from different processes of elastic or inelastic collisions which can take place in the medium. The collisions limit the lifetime of the excited level of the radiating atom, and lead also to a lorentz-type profile [15]. Especially, in our conditions, the Van der Walls broadening (due to neutral disturbers) could be estimated to 10^{-3} nm and 10^{-5} nm for the 696.5 nm Ar I and 538.3 nm Fe I lines respectively. Conditions to observed resonance broadening, that results from the collisions with energy exchange between two identical particles in different levels if one of them is connected to the ground state, are not obtained in our experimental conditions, and this type of broadening can be neglected.

The Stark broadening occurs due to the interaction of the emitter with charges particles: the resulting line profile is of lorentzian type with full-width at half-maximum $\Delta\lambda_S$ quasi-proportional to the electron density and almost independent of the plasma temperature.
Finally, the lorentzian part of the line profile may be written as:

$$\Delta\lambda_L = \Delta\lambda_N + \Delta\lambda_{vdW} + \Delta\lambda_S \quad (2)$$

and is dominated by the Stark effect because in our case

$$\frac{\Delta\lambda_N + \Delta\lambda_{vdW}}{\Delta\lambda_L} < 1\% \quad (3)$$

Doppler broadening is a consequence of atoms and ions moving in a medium of temperature T. If the velocity function distribution is supposed to be maxwellian, the line profile has a gaussian shape with the full-width at half-maximum

$$\Delta\lambda_D \cong 7.1628\times10^{-7}\ \lambda\sqrt{T/m} \qquad \text{[nm]} \quad (4a)$$

where λ is expressed in nm and m in atomic units. Then, the gaussian part of the line profile may be written as:

$$\Delta\lambda_G = \sqrt{\Delta\lambda_A^2 + \Delta\lambda_D^2}\ . \quad (4b)$$

When the temperature 11000 K, the full-width of Doppler broadening for the 696.543 nm Ar I line close to 1.15×10^{-2} nm and for the 538.33 nm Fe I line close to 1.08×10^{-2} nm. Generally, in our experimental conditions Doppler broadening may be regarded as a small correction in comparison to the one caused by the Stark effect.

In our case three broadening mechanisms should be taken into account: the Stark effect caused by electrons, the apparatus function and Doppler effect. Other contributions are much smaller.

3.2. The Abel inversion for side-on measurements

In each experiment, a thin slice of the arc column at the distance h from the cathode, was observed side-on. The image of the plasma formed by the optical system on the entrance slit of the spectrometer was rotated by 90 degrees by the Dove's prism. This way we could record on the CCD array the transversal light distribution of a thin (15 μm) plasma layer perpendicular to the arc axis at selected distance from the weld-pool. As it is well known, in order to obtain the radial distributions of a spectral line profile $\varepsilon_\lambda(r)$, from integrated along the direction of observation y measured intensity $I_\lambda(y)$, the Abel inversion procedure (inversion) should be applied [16, 17]. In this experiment, Abel inversion was only applied for the plasma

diagnostic purposes (on 696.5 nm Ar I line and 538.3 nm Fe I line – see next section) and one another of Fe I spectral line (see section 5). We paid a special attention to determination of the plasma column symmetry axis position and size. Nevertheless, our results are certainly less precise than it would be in a case of more stable and symmetric plasma source, like stabilized electric arc. For these reasons, we enlarged uncertainty limits of our results.

3.3. Plasma diagnostics

For some spectral lines, knowledge of the Stark component $\Delta\lambda_s$ of the line profile permits to determine free electrons density N_e of the plasma if the Gaussian part may be "subtracted" form the measured line profile. Spectral lines of Ar I in our plasma are broadened mainly by the Stark effect and have in principle the lorentzian profile ($\Delta\lambda_A << \Delta\lambda_S$). For the Fe I lines situation is different because the Stark broadening is comparable to the apparatus function. In this case, in order to extract the Stark component of the measured profile, we used a numerical procedure with apparatus profile previously measured.

Sola *et al.* [18, 19] applied a diagnostic method which permits to obtain simultaneously the temperature and free electrons density, without applying a hypothesis concerning the equilibrium state of the plasma. Application of this method implies the good knowledge of dependences of the Stark broadening of two spectral lines on free electron density and temperature. For this purpose we have chosen: the 696.5 nm Ar I line, corresponding to the transition 4p'[1/2]-4s[3/2], and 538.3 nm Fe I line corresponding to the e^5H-$z^5G°$ transition. These two lines are strongly broadened in the welding arc plasma and dependences of they profiles on temperature are different:

$$\begin{cases} \Delta\lambda_S^{Ar} = 0.0814_{(\pm 0.0041)} \cdot \dfrac{N_e}{10^{23}} \cdot \left(\dfrac{T_e}{13000}\right)^{0.3685} & \text{See reference [20]} \\ \Delta\lambda_S^{Fe} = 0.2648_{(\pm 0.0123)} \cdot \dfrac{N_e}{10^{23}} \cdot \left(\dfrac{T_e}{13000}\right)^{1.6700_{(\pm 0.2098)}} & \text{See references [8, 9], following [5, 21]} \end{cases} \quad (5a)$$

where : $\Delta\lambda_S^{Ar}$ and $\Delta\lambda_S^{Fe}$ are in nm, N_e in m^{-3}, and T_e in K (the underscripts correspond to the uncertainties on the coefficients given in the references [20] and [8], for the argon and iron lines respectively). In these conditions, if we can measure $\Delta\lambda_S^{Ar}$ and $\Delta\lambda_S^{Fe}$ in the same point r of the plasma column, we have:

$$T_e(r) = 13000 \cdot \left(0.3074_{(\pm 0.0298)} \times \frac{\Delta\lambda_S^{Fe}}{\Delta\lambda_S^{Ar}}\right)^{0.7683_{(\pm 0.1239)}} \quad (5b)$$

Then, it is easy to obtain $N_e(r)$ using one of the equations (5a). The plasma diagnostics procedure as well as discussion of results may be found in our previous paper [7, 8, 9].

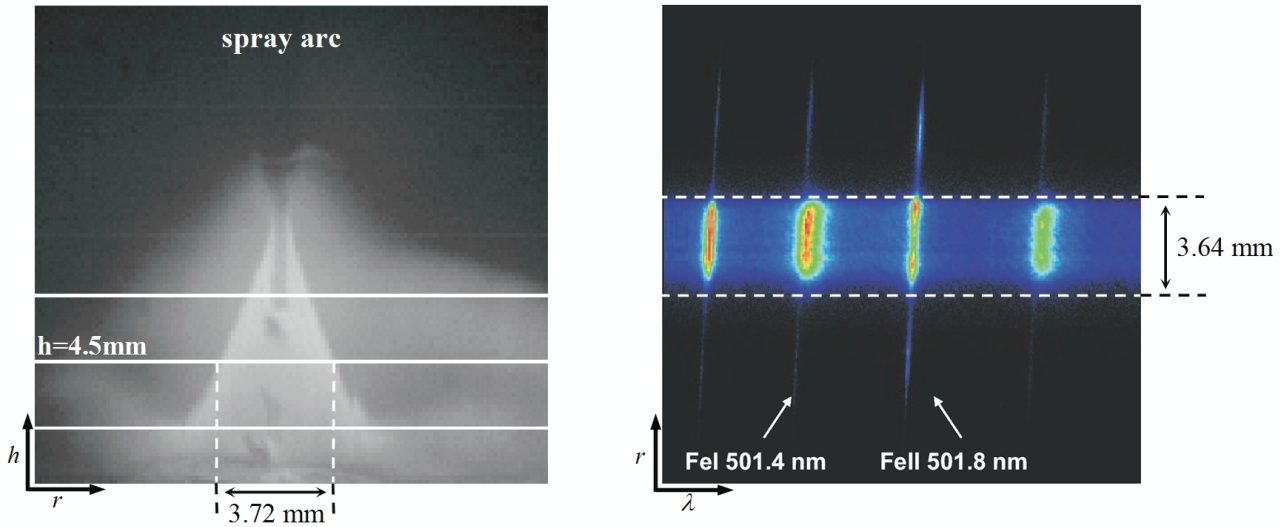

Figure 6 – Comparison between one photo of the welding arc and the emission spectrum of plasma.

4. Measurement of the Stark width and shift for some Fe I and Mn I lines.

When pure argon was used as the shielding gas, we observed unusual distribution of emitted spectral lines. As we may see on the picture taken be the fast camera (see figure 3 and figure 6) the arc plasma was composed of two zones. The bright one in the centre has the form of a cone and is surrounded by a peripheral zone of much smaller brightness. In the bright zone of discharge spectral lines of metals (Fe, Mn, Co, Cu) were very intense, strongly broadened and shifted. In the outside zone the same lines were very narrow, not shifted and weaker (figure 6). Like we can see on figure 6, the width of the bright zone in the picture recorded by the fast camera corresponds almost exactly to the height of the Fe line from the CCD camera (the image of the discharge was rotated by 90^0).

We noticed on pictures taken by CCD camera that for both zones, Fe I spectral lines width and position seem to be rather independent of the distance from the arc centre, as in case of lines emitted from uniform plasma. Transition between zones takes place at very short distance in comparison with dimensions of both zones. It may be observed in figure 7 where the Stark width and position of the line centre for the 485.97 nm Fe I line are shown. The half-width and position of line were determined without the Abel transformation.

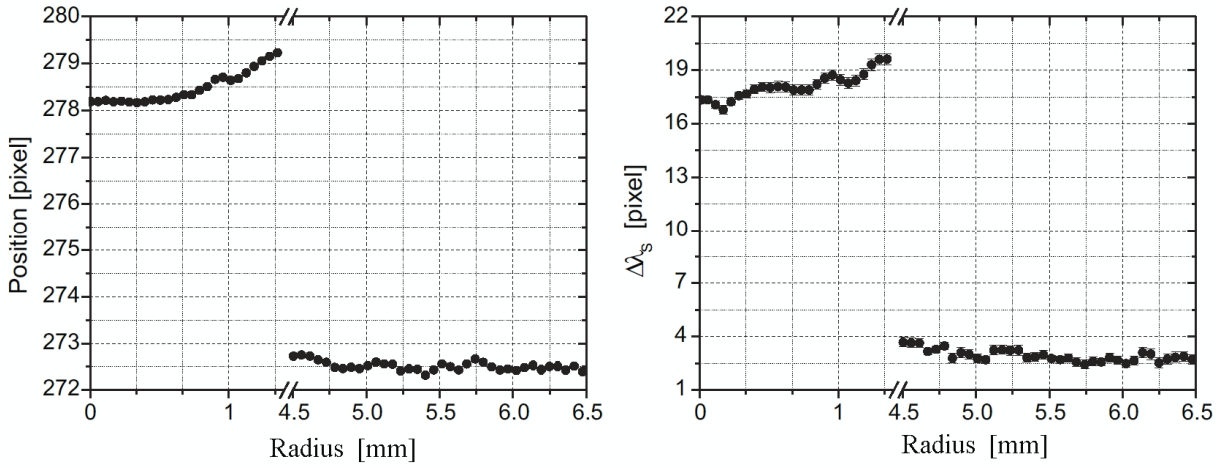

Figure 7 – Radial distribution of the Stark half-width and position of the maximum of line profile for the 485.97 nm Fe I line at $h \approx 4.5$ mm from the cathode, obtained without applied the Abel inversion procedure. [Experimental conditions: Pure argon; $I_{arc} \approx 330$ A; $U_{arc} \approx 32$ V; $v_{wire} = 9$ m.mn^{-1}]

For the plasma layer of the plasma observed in this experiment we determined the radial distribution of temperature and free electrons density (figure 8). Description of applied plasma diagnostic method and results may be found in [7, 8, 9]. It may be noticed that in the bright zone (shadowed in the figure 8b) the free electron density is almost the same and temperature changes very little, what gives as a result quite the same Stark half-with of line profile.

Pictures recorded by the fast camera (figure 3) and spectrum obtained with CCD camera (figure 8a), the measured radial distribution of free electrons concentration (figure 8b) and dependences shown in figure 7, indicate that inside the bright zone we have almost uniform plasma suitable for measurements of Stark parameters. Intense spectral lines of metallic plasma components contain only a small contribution of the same lines emitted form the outside zone, which are much weaker, narrower and not shifted.

Taking into account all these reasons, we were able to measure Stark widths and shifts for several spectral lines of Mn I and Fe I. We found the plasma region between 0.82 to 1.35 mm from the arc axis, what corresponds to 10 pixels of detector, as the most suitable for our measurements. For this plasma region, differences between results for the 538.3 nm Fe I line, with and without the Abel inversion did not exceed 2%.

Possibility of registration of a spectral line profile far away from the arc axis, were temperature and free electrons concentration were much smaller then in the centre, allowed us to measure spectral lines shift. Supplementary motivation was lack of such data for Mn I and very few results for Fe I in the literature.

For each experiment CCD camera registered the same spectrum fifteen times during stable phase of plasma discharge. For calculation of Stark parameters we used ten added spectra, what permits to improve a signal to noise ratio. Measurements were performed for 15 Mn I and 11 Fe I spectral lines. We measured only lines strong enough far away from the arc centre, for which a good quality Voigt profile could be fitted.

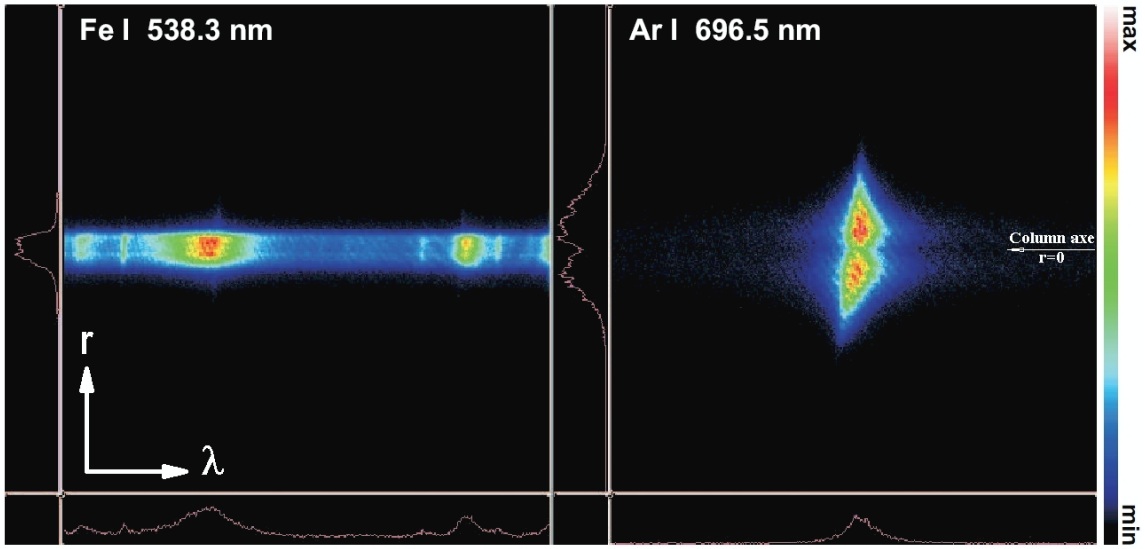

a/ Recorded spectra

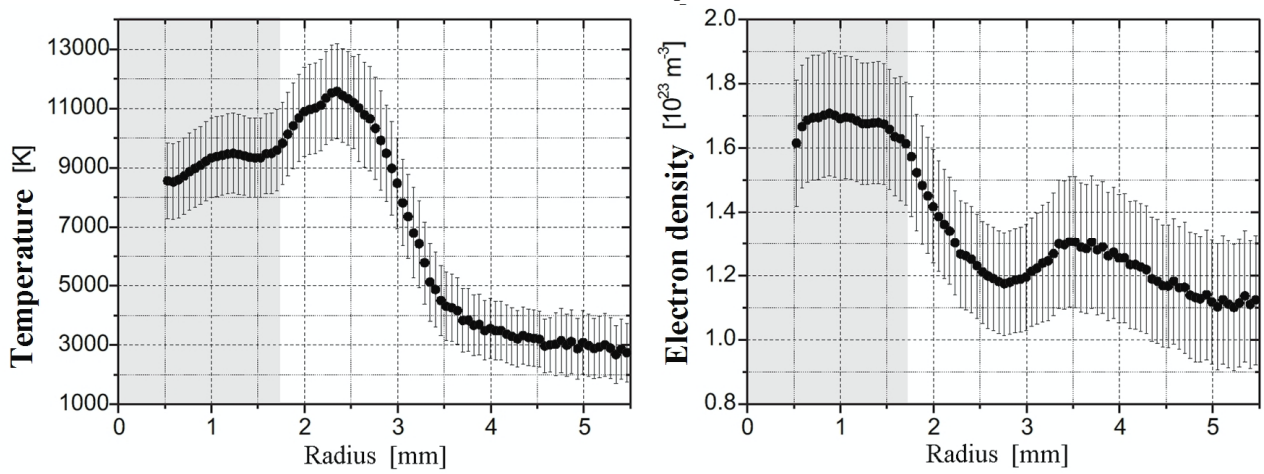

b/ Radial distributions of temperature and electron density

Figure 8 – Pure Argon - h≈4.5 mm from the cathode / Spray mode
[Experimental conditions: Pure argon; I_{arc} ≈ 330 A; U_{arc} ≈ 32 V; v_{wire} = 9 m/mn]

Using known $T_e(r)$, the Doppler width for a line was calculated. As the apparatus function was known (measured), the gaussian contribution to the measured spectral lines could be subtracted from the measured profiles. Voigt's profile was fitted to the measured line profile with known gaussian component. As a result, the lorentzian part of the Voigt profile was determined as well as position of the line maximum.

Data on the lifetimes of levels of FeI and MnI are not complete, and it is difficult to estimate the natural broadening of the analyzed spectral lines. However, based on the conclusions of O'Brien [13], we may assume that the natural broadenings are around 10^{-5} nm and can be neglected. Moreover, for all the lines considered, none of the transition levels is in resonance with the ground state: it is therefore quite justified to neglect the influence of the resonance broadening on the width of the emission lines. Then, we have not taken into account the influence of van der Waals effect, which induces a broadening within the measurement uncertainties.

Finally, value of the lorentzian component of the total half-width was taken as a good approximation of the Stark width. Difference of position of the line, for far away and near centre zones, was taken as the line shift for given T_e and N_e. With exception of the 542.41 nm Fe I line for which we decide to study the dependence of normalized Stark width as a function of temperature (see next section), data were not processed with Abel inversion.

Resonance transitions, with large transition probability, were strongly reabsorbed; for this reason we eliminated from measurements not only resonance transition but also other ones which could be suspected for self-absorption. For selected lines there is no direct way to determine possible degree of self-absorption.

Thus, we applied a numerical method which consists on fitting a Voigt profile to experimental data twice. First fit is calculated for all measured points, for the second fit points close to the line maximum (above half-maximum) are not taken into calculation. Results of this procedure for the 538.34 nm Fe I line are shown in figure 9.

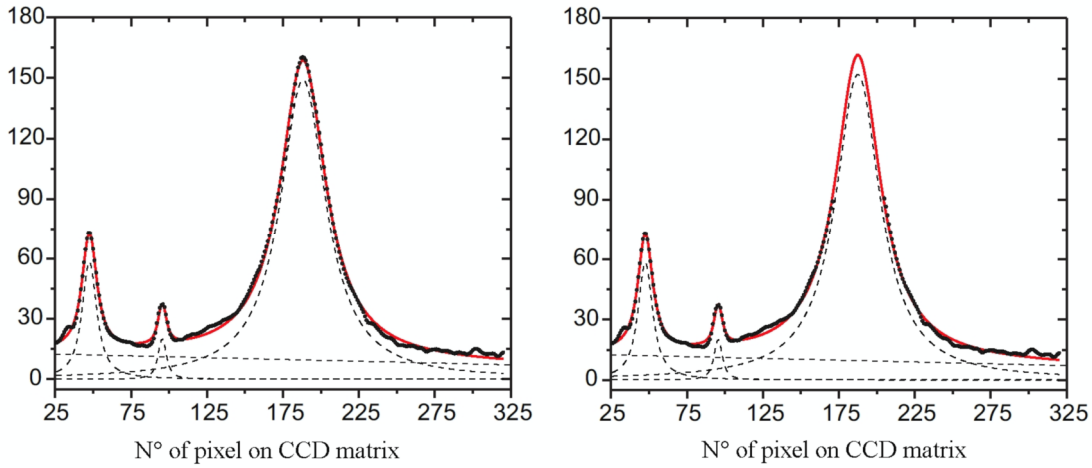

Figure 9 – The part of recorded spectrum obtained for h=4.5 mm show three emission lines: 537.76 nm Mn I, 537.96 nm Fe I and 538.34 nm Fe I (in arbitrary units). The left figure shows the Voigt profiles fit to all experimental points. The right figure shows results of similar fit when points in the central part of the 538.34 nm Fe I line were not taken to calculation. Difference for half-width was below 1.5%. Self-absorption for Mn I lines is much smaller because the content in the wire electrode is about 100 times smaller in comparison with the Fe atoms concentration.

Complete discussion on the data evaluation can be found in references [7-9]. Values of concentration of free electrons, temperature, Stark half-width, and position of the line profile maximum were determined for as weighted averages for 10 points (pixels) at the distance from the arc axis from 0.82 mm to 1.35 mm. Statistical errors of these values were calculated as the standard deviation. In the case of $\Delta\lambda_S$ and $\Delta\lambda_D$ errors were enlarged with uncertainties coming from numerical procedures and reproducibility of the plasma condition for independent experiments. The Stark shifts were calculated with assumption that lines in the second zone, far away from the arc center were not shifted. An uncertainties coming from this assumption is not larger than 5%.

Statistical errors of T_e and N_e are not large and equal to 4.5% and 3.5%, respectively. However, we should take into consideration uncertainties of the plasma diagnostics, especially taking into account the systematic errors linked to the used coefficients introduced in equations (5a) and (5b). Then, as it was discussed in [7, 8, 9], uncertainties of these values are not larger than 15% and 20%, respectively. Results of our measurements are shown in table 1, for Mn I lines and table 2 for Fe I transitions.

λ [nm]	Transition	Multiplet	J_j - J_k	E_j - E_k [eV]	$\Delta\lambda_S$ [10^{-2} nm]	d_S [10^{-2} nm]
446.47	$3d^6\,(^5D)\,4s - 3d^6\,(^5D)\,4p$	$a^4D - z^4D^o$	5/2 – 5/2	2.920 - 5.696	3.22±0.36	0.75±0.12
447.01			3/2 – 3/2	2.941 - 5.714	2.91±0.32	
447.28			1/2 – 1/2	2.953 - 5.724	2.78±0.31	
449.01			1/2 – 3/2	2.953 - 5.714	2.74±0.31	
449.89			3/2 – 5/2	2.941 - 5.696	2.86±0.31	
450.22			5/2 – 7/2	2.920 - 5.673	3.12±0.35	
475.40	$3d^5\,(^6S)\,4s\,4p\,(^3P^o) – 3d^5\,4s\,(^7S)\,5s$	$z^8P^o - e^8S$	5/2 – 7/2	2.282 - 4.889	11.1±1.1	4.08±0.62
478.34			7/2 – 7/2	2.298 - 4.889	11.5±1.3	4.38±0.66
482.35			9/2 – 7/2	2.319 - 4.889	12.6±1.4	4.42±0.67
476.15	$3d^6\,(^5D)\,4s - 3d^6\,(^5D)\,4p$	$a^4D - z^4F^o$	1/2 – 3/2	2.953 - 5.556	2.59±0.29	0.48±0.07
476.24			7/2 – 9/2	2.888 - 5.491	4.25±0.47	0.58±0.09
476.59			3/2 – 5/2	2.941 - 5.542	2.80±0.31	0.50±0.08
476.64			5/2 – 7/2	2.888 - 5.520	3.51±0.39	0.56±0.09
542.04	$3d^6\,(^5D)\,4s - 3d^5\,(^6S)\,4s\,4p\,(^1P^o)$	$a^6D - v^6P^o$	7/2 – 5/2	2.143 - 4.429	3.57±0.41	0.56±0.11
551.68			3/2 – 3/2	2.178 - 4.425	2.79±0.31	

Table 1 – Stark full-width at half-maximum $\Delta\lambda_S$ and displacements Stark d_S of Mn I spectral lines determined for $N_e = 1.69\times10^{23}$ m^{-3} et T_e = 9325 K - $\Delta N_e/N_e \leq 20\%$ and $\Delta T_e/T_e \leq 15\%$

λ [nm]	Transition	Multiplet	J_j - J_k	E_j - E_k [eV]	$\Delta\lambda_S$ [10^{-2} nm]	d_S [10^{-2} nm]
446.66	$3d^7$ (a^4P) 4s – $3d^6$ (a^3P) 4s 4p ($^3P°$)	$b^3P – x^3D^o$	2 – 3	2.832 - 5.607	2.73±0.31	0.15±0.03
478.68	$3d^7$ (a^2P) 4s – $3d^6$ (a^3P) 4s 4p ($^3P°$)	$c^3P – x^3D^o$	2 – 3	3.017 - 5.607	1.19±0.23	
478.88	$3d^7$ (a^2H) 4s – $3d^6$ (^3H) 4s 4p ($^3P°$)	$b^3H – z^3H^o$	6 – 6	3.237 - 5.825	1.34± 0.19	
478.97	$3d^7$ (a^2D) 4s –	$a^1D – z^1D^o$	2 – 2	3.547 - 6.134	1.77±0.20	0.48±0.02
485.97	$3d^6$ (^5D) 4s 4p ($^3P°$) – $3d^6$ (^5D) 4s (^6D) 5s	$z^7F^o – e^7D$	2 – 1	2.876 - 5.426	7.55±0.85	2.59±0.39
501.49	$3d^6$ (^5D) 4s 4p ($^3P°$) – $3d^6$ (^5D) 4s (^4D) 5s	$z^3F^o – e^3D$	3 – 2	3.943 - 6.415	7.99±0.89	2.57±0.39
502.22			2 – 1	3.984 - 6.452	7.91±0.88	2.53±0.39
556.96	$3d^6$ (^5D) 4s 4p ($^3P°$) – $3d^6$ (^5D) 4s (^4D) 5s	$z^5F^o – e^5D$	2 – 1	3.417 - 5.642	10.9±1.2	3.22±0.48
557.28			3 – 2	3.397 - 5.621	12.6±1.4	3.59±0.43
557.61			1 – 0	3.430 - 5.653	10.8±1.2	3.04±0.46

Table 2 – Stark full-width at half-maximum $\Delta\lambda_S$ and displacements Stark d_S of Fe I spectral lines determined for $N_e = 1.69\times10^{23}$ m^{-3} et T_e = 9325 K - $\Delta N_e/N_e \leq 20\%$ and $\Delta T_e/T_e \leq 15\%$

5. Temperature dependence of the 542.4 nm Fe I line normalized Stark width at $N_e=10^{23}$m^{-3}.

The 542.41 nm Fe I line, corresponding to transition $3d^7(^4F)4d \rightarrow 3d^7(^4F)4p$, belongs to the multiplet ($e^5H \rightarrow z^5G$), the same as for the 538.34 nm Fe I line applied to the plasma diagnostics: their characteristics are given in the Table 3. Taking into account regularities of Stark parameters among lines of the multiplet [22-25], we decided to check consistency of our results by comparing Stark dependence of normalized Stark width as the function of temperature.

Data for the 542.41 nm Fe I line were elaborated the same way, with the Abel transformation and fit of the Voigt profile, as for the 538.34 nm Fe I line. The dependence of the normalized Stark width for the investigated line on the temperature is shown in figure 10. The Stark shift for this line was determined with previously described procedure.

λ [nm]	Transition	Multiplet	J_j - J_k	E_j - E_k [eV]
538.34	$3d^7$ (^4F) 4p - $3d^7$ (^4F) 4d	$z^5G° – e^5H$	5 – 6	4.313 – 6.615
542.41	$3d^7$ (^4F) 4p - $3d^7$ (^4F) 4d	$z^5G° – e^5H$	6 – 7	4.320 – 6.606

Table 3 – Characteristics of Fe I line transitions

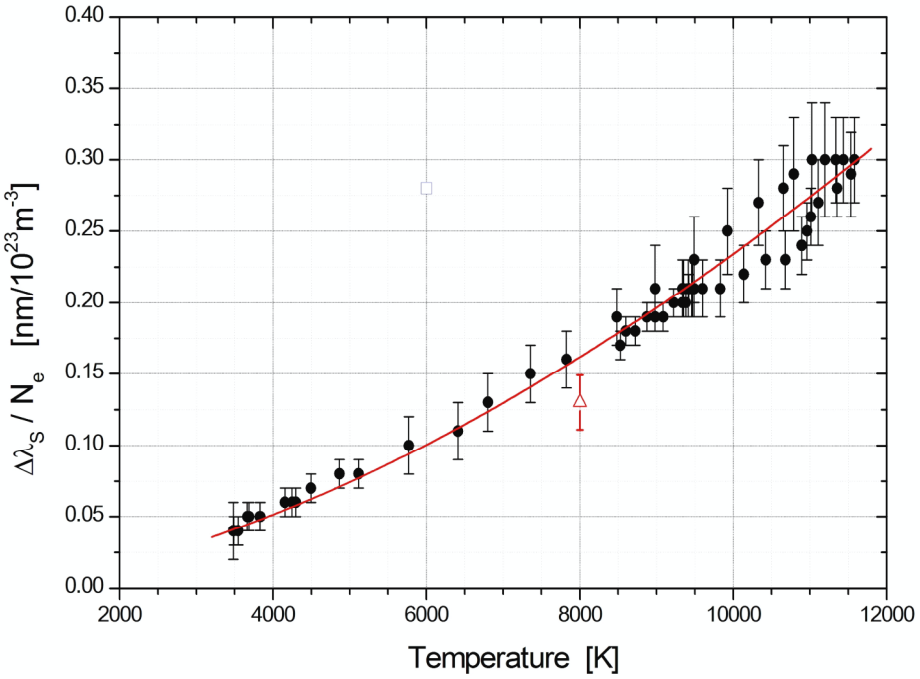

Figure 10 – Normalized Stark width of the 542.4~nm Fe I spectral line as a function of temperature. (● - this work ; Δ - value obtained from Moity [26] ; □ - value obtained from Fructos [in 5])

The numerical adjustment of these last data to a power function leads to the following equation (cf. dotted line on figure 10):

$$\Delta\lambda_S^{Fe} = 0.3612 \cdot \frac{N_e}{10^{23}} \cdot \left(\frac{T_e}{13000} \right)^{1.6551} \quad (6)$$

where : $\Delta\lambda_S^{Fe}$ is in nm, N_e in m^{-3}, and T_e in K. The calculated values for the exposure (1.6551) and the proportionality factor (0.3612) are comparable to that obtained for the 538.34 nm Fe I spectral line (1.6700 and 0.2648 respectively - cf eq. (5)).

Moity [26] has analyzed the evolution of Stark broadenings $\Delta\lambda_S$ of the Fe I spectral lines according to the electronic density N_e for temperature of 8000 K. He carried out its measurements by using a discharge of the shock-tubes type in a mixture of neon with 5% of iron-pentacarbonyl $Fe(CO)_5$ and 10% to 40% of xenon, according to the concentration of free electrons wished. Considering dependence like:

$$\Delta\lambda_S^{Fe} = 7.51\times10^{-8} \cdot \lambda^2 \cdot C_4^{2/3} \cdot N_e \qquad [cgs] \quad (7)$$

He determined the Stark constants C_4 for twenty lines of atomic iron. In particular, he proposed for the 542.41 nm Fe I spectral line, $C_4=1.42\times10^{-14}$ $cm^4.s^{-1}$ with accuracy of 22%. Applying these results to the temperature of 8000 K and electron density close to 10^{23} m^{-3}, we obtain $\Delta\lambda_S = (13.0\pm1.9)\times10^{-2}$ nm: This value is in agreement, within the limit of measurement uncertainties, with our results (cf. Figure 10).

Under their measurement conditions (T_e=6000 K, N_e==10^{22} m^{-3}), Fructos *et al.* (reference [2] in the last compilation of the NIST [5]) obtain $\Delta\lambda_S$ = 0.028 nm (FWHM) and d_S=-0.007 nm for the 542.41 nm Fe I line, i.e.

$$\frac{\Delta\lambda_S^{Fe}}{N_e} = 0.28 \quad \left[\frac{nm}{10^{23}\ m^{-3}} \right] \quad (8)$$

This value is considerably different from that which we obtained. It should besides be noted that the analysis of the results published by these same authors in the same source, for other spectral lines (538.34 nm, 541.5 nm, 541.1 nm), clearly shows a similar tendency: normalized Stark broadening proposed by the authors, are considerably higher than those obtained for example by Lesage [21] at higher temperatures. Then, it is probable that it is necessary to take into account the introduction of a systematic error in their results.

6. Conclusion

Investigation of metallic elements emission spectra is difficult because of problems with introduction of metal atoms into plasma sources, uniform or with an axial symmetry, suitable for spectroscopic measurements. This is the main reason of pour knowledge of Stark parameters for these kinds of spectral lines. At the same time, knowledge of the atomic constants is important for many applications in laboratories as well as in astrophysics. The GMAW plasma was not yet considered as a light source suitable for the Stark parameters measurement. Results of our measurements show that special properties of the MIG plasma may be useful in this domain because composition of the wire-electrode may be easily adapted to needs of an experiment.

7. Acknowledgement

This work was supported in part by Air Liquide, Saint Ouen l'Aumone (France).

8. Bibliography

1 Konjevic M and Wiese W L 1976 ,,Experimental Stark widths and shifts for non - hydrogenic spectral lines of ionized atoms" *J.Phys.Chem.Ref.Data* **5** 259

2 Konjevic M, Dimitrijevic M S and Wiese W L 1984 ,,Experimental Stark Widths and Shifts for Spectral Lines of Neutral Atoms (A Critical Review of Selected Data for the Period 1976 to 1982)" *J.Phys.Chem.Ref.Data* **13** 619

3 Konjevic M, Dimitrijevic M S and Wiese W L 1984 ,,Experimental Stark Widths and Shifts for Spectral Lines of Positive Ions (A Critical Review and Tabulation of Selected Data for the Period 1976 to 1982)" *J.Phys.Chem.Ref.Data* **13** 649

4 Konjevic M and Wiese W L 1990 „Experimental Stark widths and shifts for spectral lines of neutral and ionized atoms" *J.Phys.Chem.Ref.Data* **19** 1307

5 Konjevic N, Lesage A, Fuhr J R and Wiese W L 2002 „Experimental Stark Widths and Shifts for Spectral Lines of Neutral and Ionized Atoms (A Critical Review of Selected Data for the Period 1989 Through 2000)" *J.Phys.Chem.Ref.Data* **31** 819

6 Valensi F, Pellerin S, Boutaghane A, Dzierzega K, Zielinska S, Pellerin N and Briand F, 2010, *J. Phys. D (this issue)*

7 Valensi F 2007 „Contribution à l'étude des phénomènes liés aux effets anodiques et cathodiques en soudage MIG-MAG" PhD Thesis, University of Orléans (France) *(in french language)*

8 Zielinska S, Musioł K, Dzierzega K, Pellerin S, Valensi F, de Izarra C and Briand F 2007 „Investigations of GMAW plasma by optical emission spectroscopy" *Plasma Sources Sci. Technol.* **16** pp.832–838

9 Zielinska S 2005 „Propriétés physiques du plasma MIG-MAG" PhD Thesis, University of Orléans (France) and Jagielonian University of Cracow (Poland) *(in french or polish languages)*

10 Zielinska S, Pellerin S, Valensi F, Dzierzega K, Musiol K, de Izarra Ch and F.Briand 2008 „Gas influence on the arc shape in MIG-MAG welding" *Eur.Phys.J. Appl.Phys.* **43**-1 111-122

11 „NIST physical reference database", http://physics.nist.gov

12 Allen C W 1964 „Astrophysical quantities" University of London, The Ath-lone Press, Second edition

13 O'Brian T R, M. E. Wickliffe M E, Lawler J E, Whaling W and Brault J M 1991 „Lifetimes, transition probabilities, and energy level in FeI",J.Opt.Am.B **8** 1185-1201

14 Pokrzywka B 2003 „Równowagowe i spektroskopowe wlasnosci plazmy w sasiedztwie katody luku elektrycznego", Wydawnictwo Naukowe Akademii Pedagogicznej, Kraków (in polish)

15 Pellerin S 1994 „Etude de la région cathodique d'un arc soufflé. Déterminations des probabilités de transition et élargissements Stark de raies d'argon II", PhD Thesis, University of Orléans (France) *(in french language)*

16 Pellerin S, Pokrzywka B, Musiol K and Chapelle J 1994 "Investigation of a cathode region of an electric arc" *J.Phys.D* **27**-3 522-528

17 Pellerin S, Musiol K and Chapelle J 1997 „Measurement of atomic parameters of many singly ionized argon lines - I. Experimental process" *J.Q.S.R.T.* **57**-3 349-357

18 Sola A, Gamero A, Cortino J, Saez M, Lao C, Calzada M D, Quintero M C and Ballesteros J 1991, ICPIG XX Barga (Italy, 5-12 July 1991) Book of Contributed Papers p.1147

19 Torres J, Jonkers J, van de Sande M. J, van der Mullen J. J. A. M, Gamero A and Sola A 2003 „An easy way to determine simultaneously the electron density and temperature in high-pressure plasmas by using Stark broadening" *J.Phys.D* **36**-13 L55-L59

20 Pellerin S, Musiol K, Pokrzywka B and Chapelle J 1996 „Stark width of 4p'[1/2]-4s[3/2]° Ar I transition (696.543 nm)" *J.Phys.B* **29** 3911-3924

21 Lesage A, Lebrun J L and Richou J 1990 „Temperature dependence of Stark parametres for FeI lines" *The Astrophysical Journal* **360** 737-740

22 Dimitrijevic M S 1982 „On the variation of Stark line width within a su-permultiplet" *Astronomy & Astrophysics* **112** 251

23 Puric J, Cuk M and Lakicevic I S 1985 „Regularities and systematic trends in Stark broadening and shift parameters of spectral lines in plasma" *Phys.Rev.A* **32** 1106

24 Puric J, Cuk M, Dimitrijevic M S and Lesage A 1991 „Regularities of Stark parametres along the periodic table" *The Astrophysical Journal* **382** 353

25 Puric J, Miller M H and Lesage A 1993 „Electron impact broadening parameters predictions from regularities : FeI, FeII, FeIII, FeIV, CIV, and SiIV" *The Astrophysical Journal* **416** 825

26 Moity J, Pieri P E and Richou J 1975 „Détermination expérimentale des constantes Stark de quelques transitions visibles de l'atome FeI" *Astronomy & Astrophysics* **45** 417-423

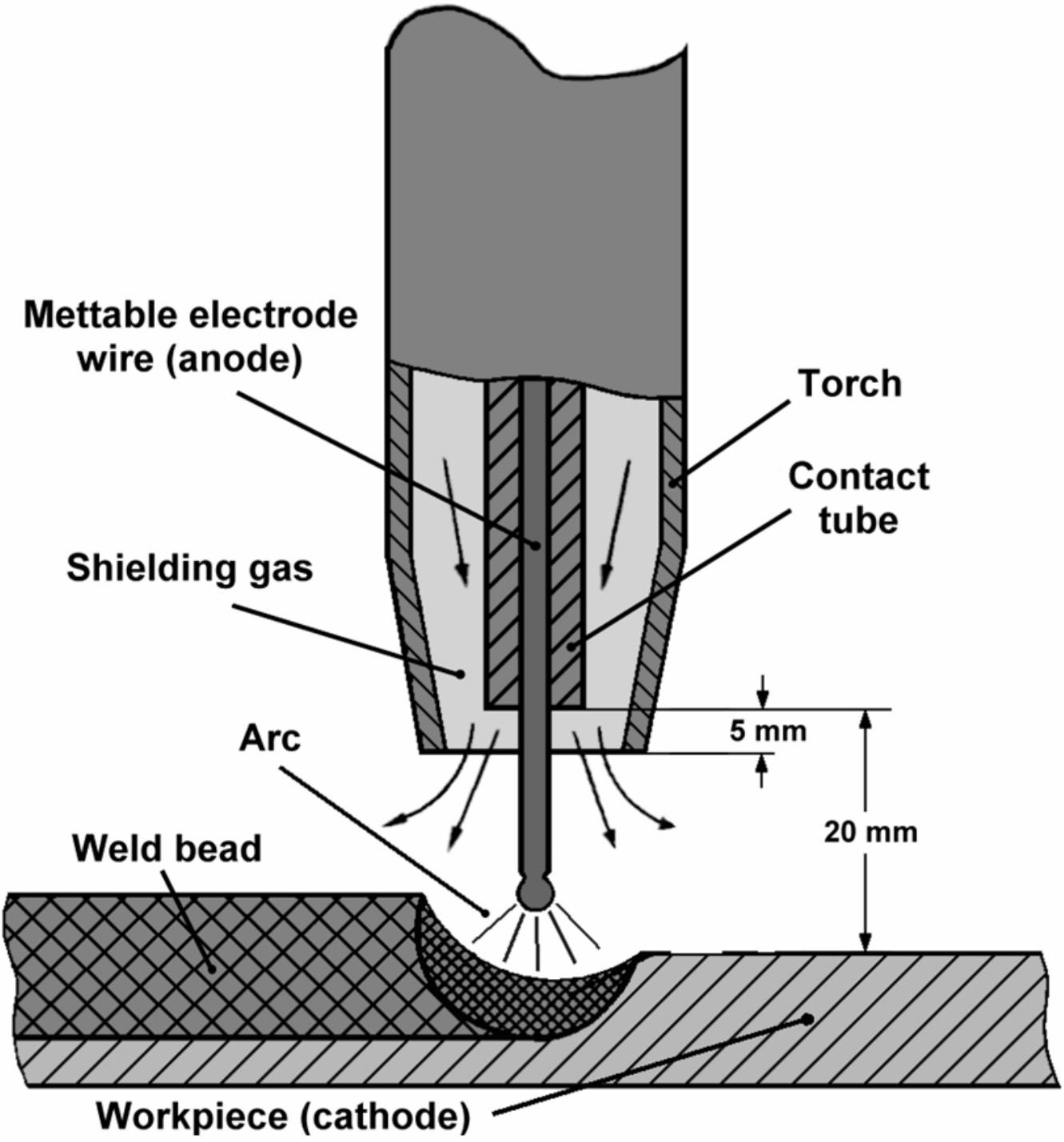

Figure 1 (Art_Wel04 Fig-01.jpg)

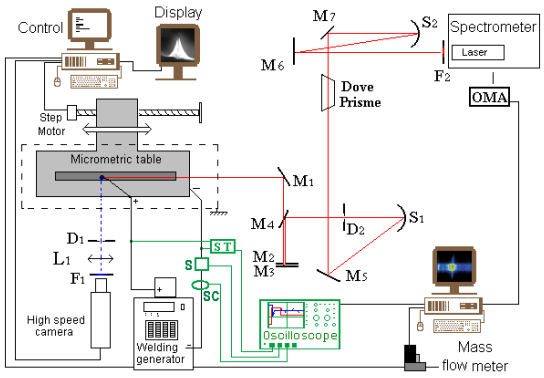

Figure 2 (Art_Wel04 Fig-02.bmp)

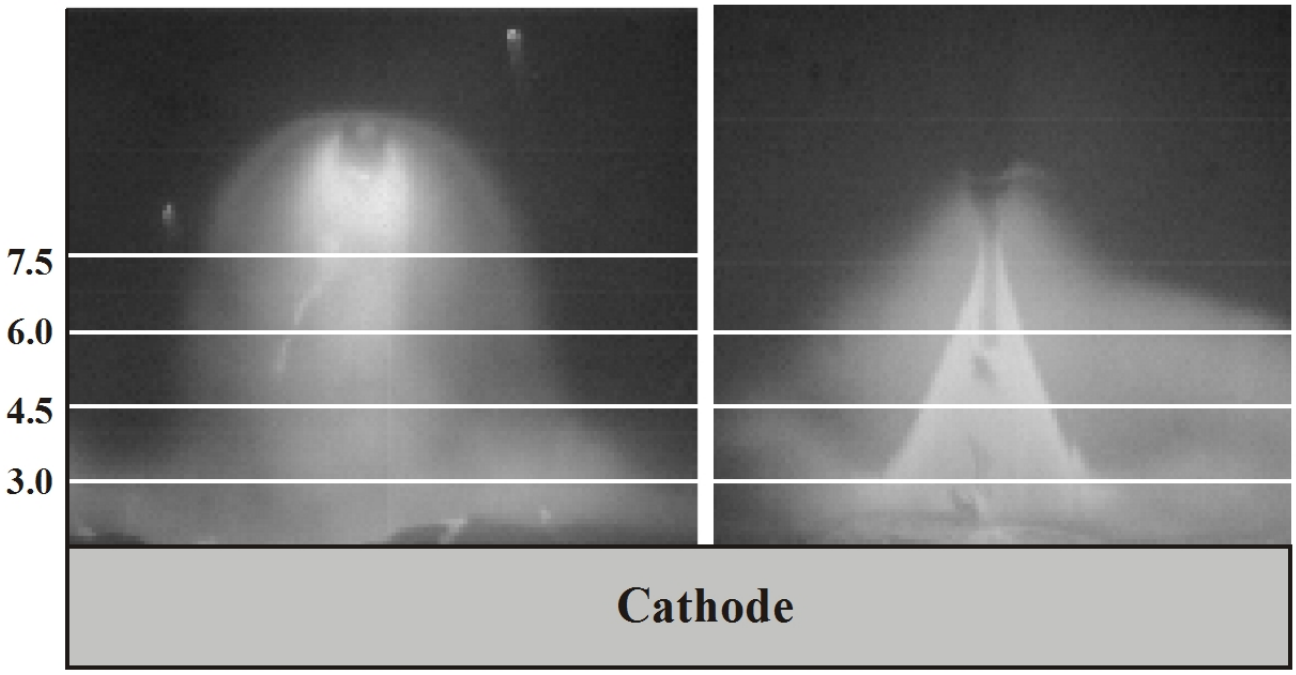

Figure 3 (Art_Wel04 Fig-03.jpg)

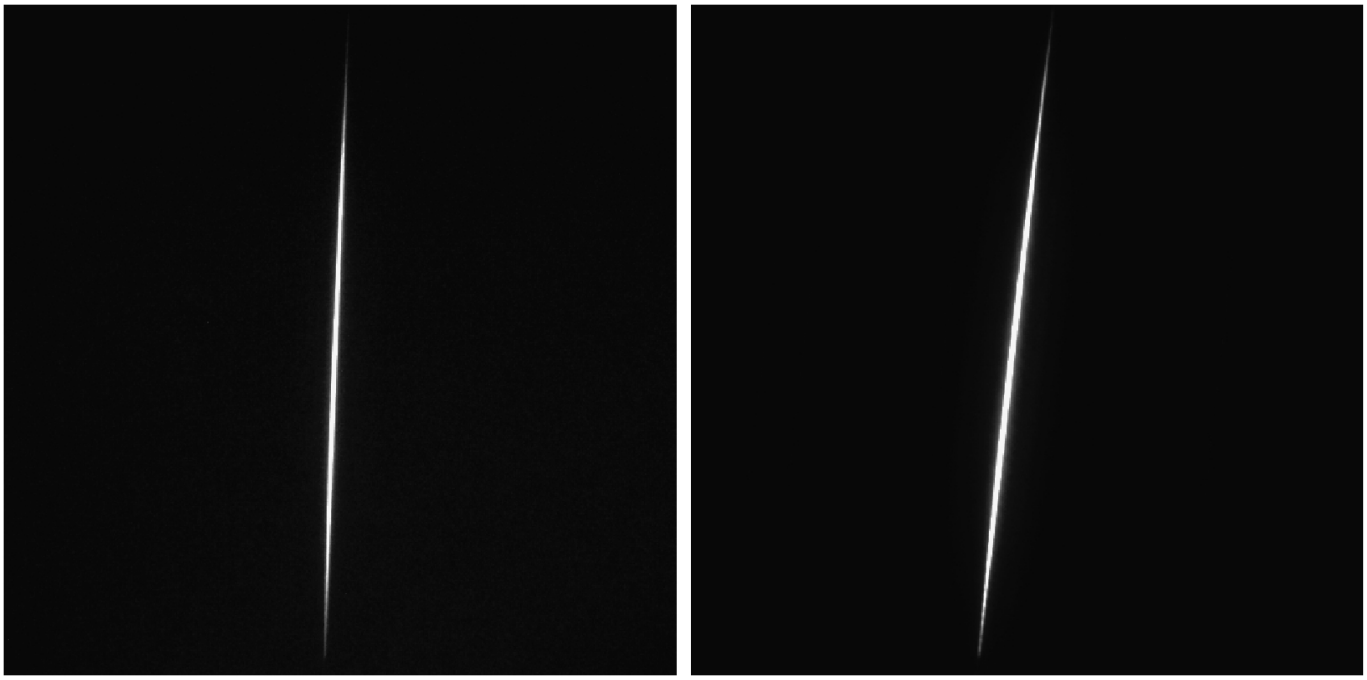

Figure 4 (Art_Wel04 Fig-04.jpg)

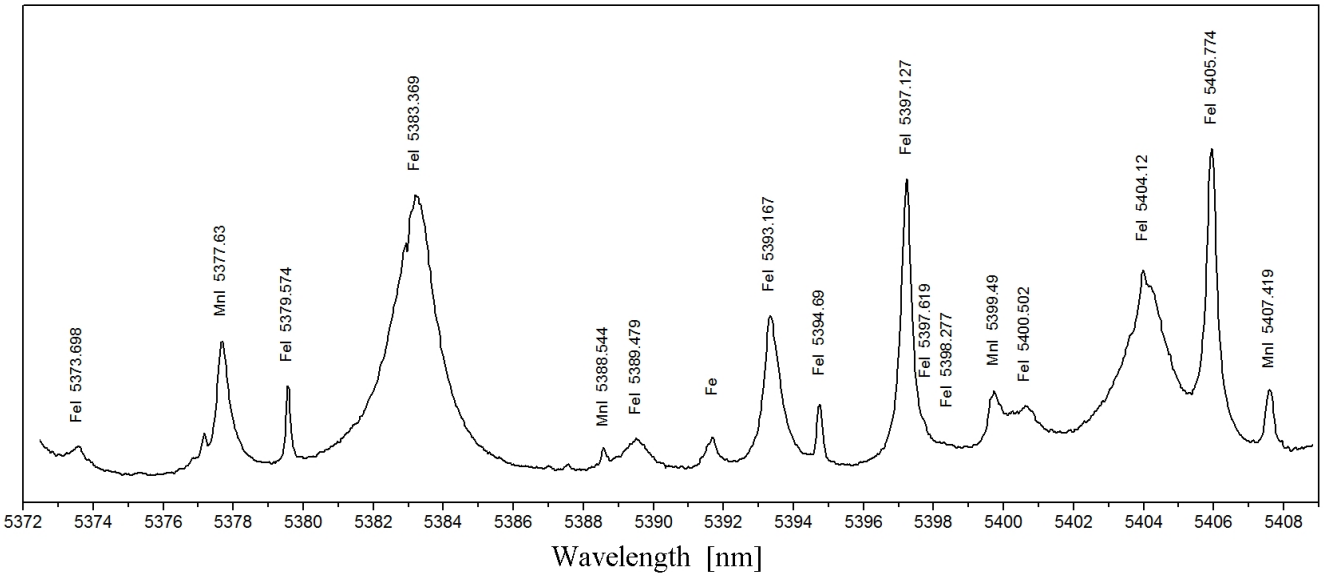

Figure 5 (Art_Wel04 Fig-05.jpg)

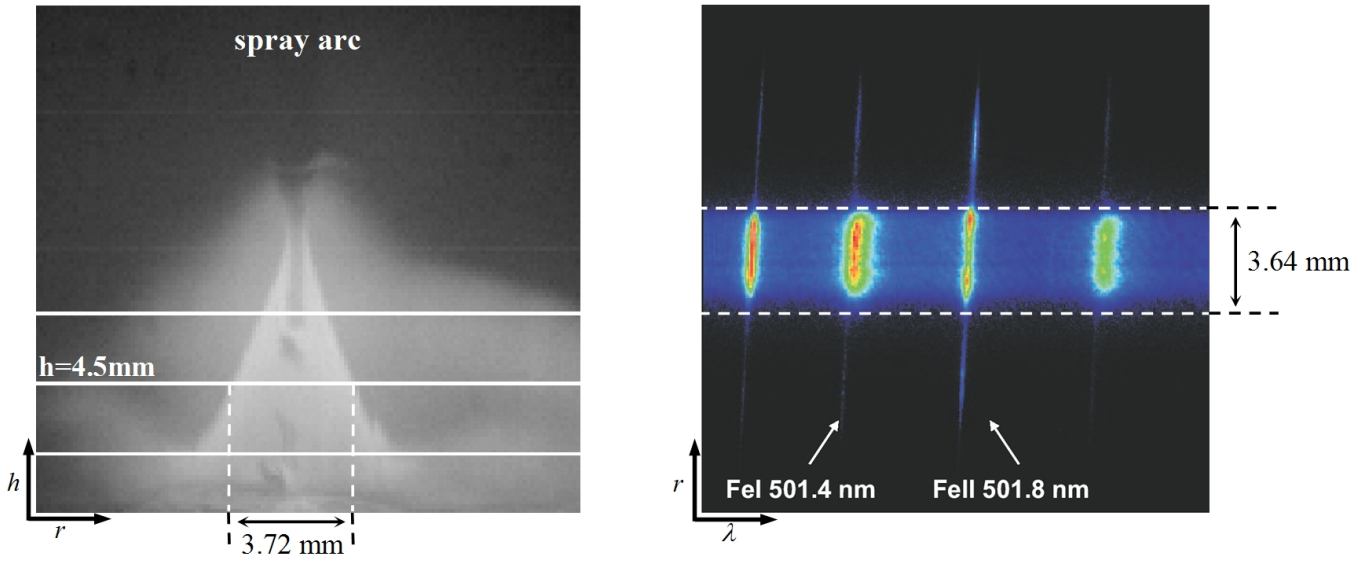

Figure 6 (Art_Wel04 Fig-06.jpg)

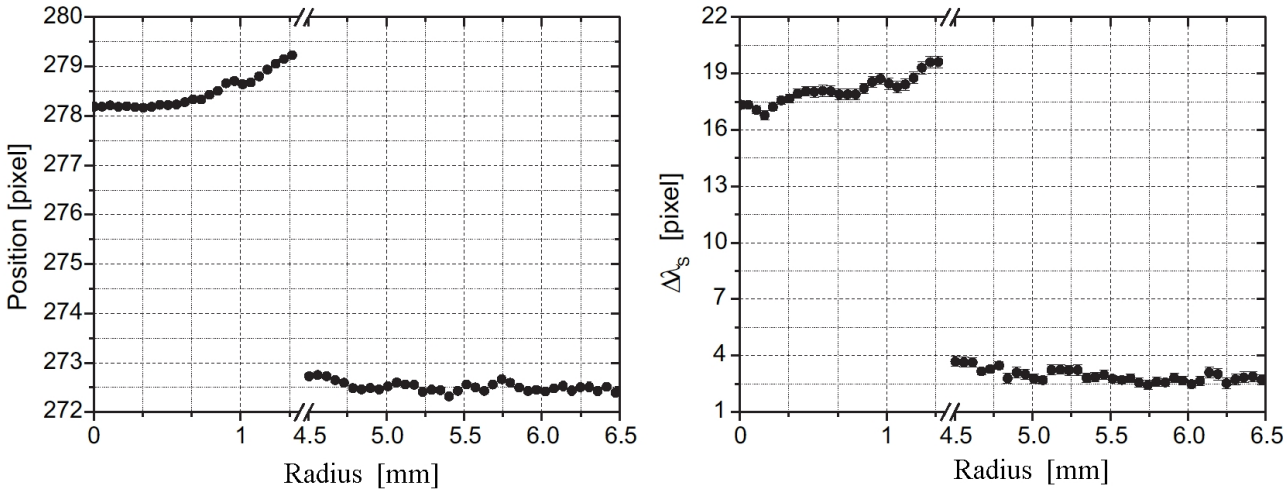

Figure 7 (Art_Wel04 Fig-07.jpg)

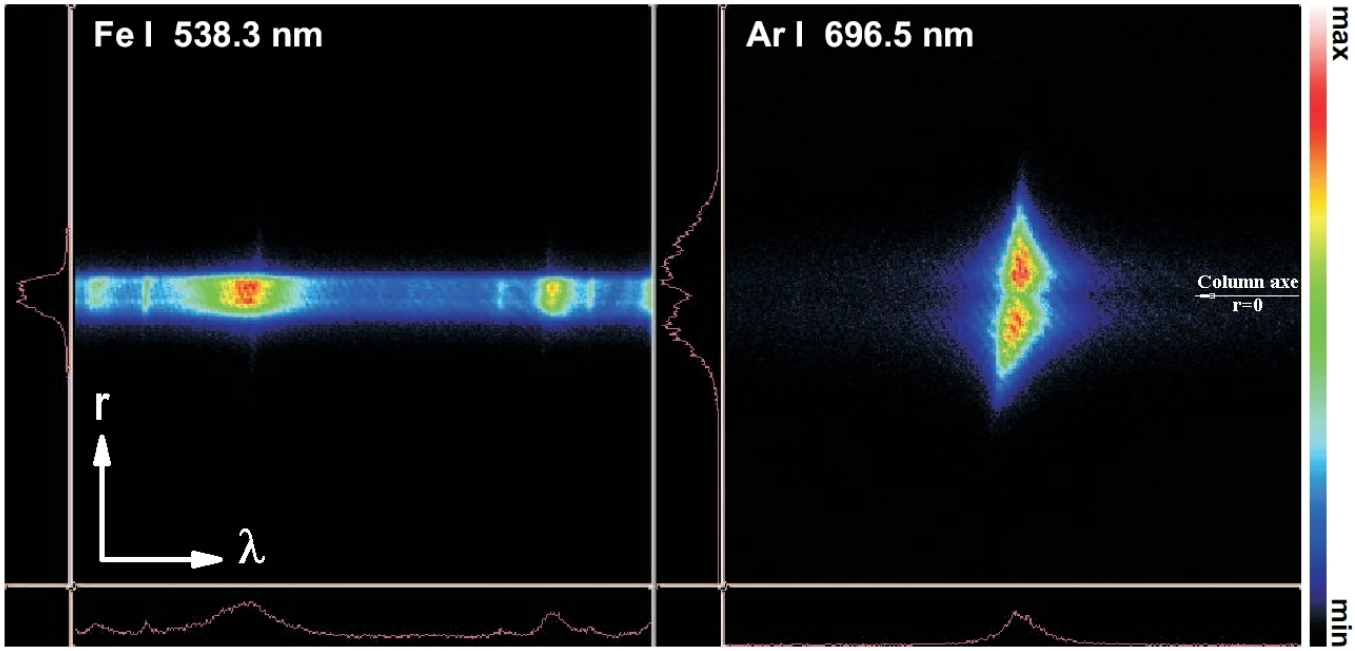

Figure 8a (Art_Wel04 Fig-08a.jpg)

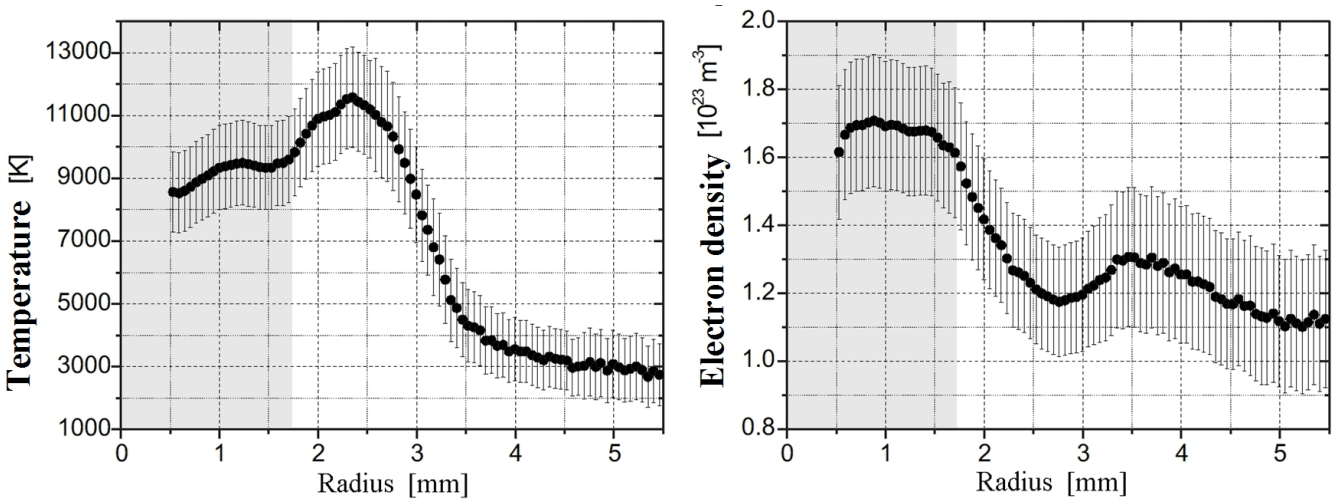

Figure 8b (Art_Wel04 Fig-08b.jpg)

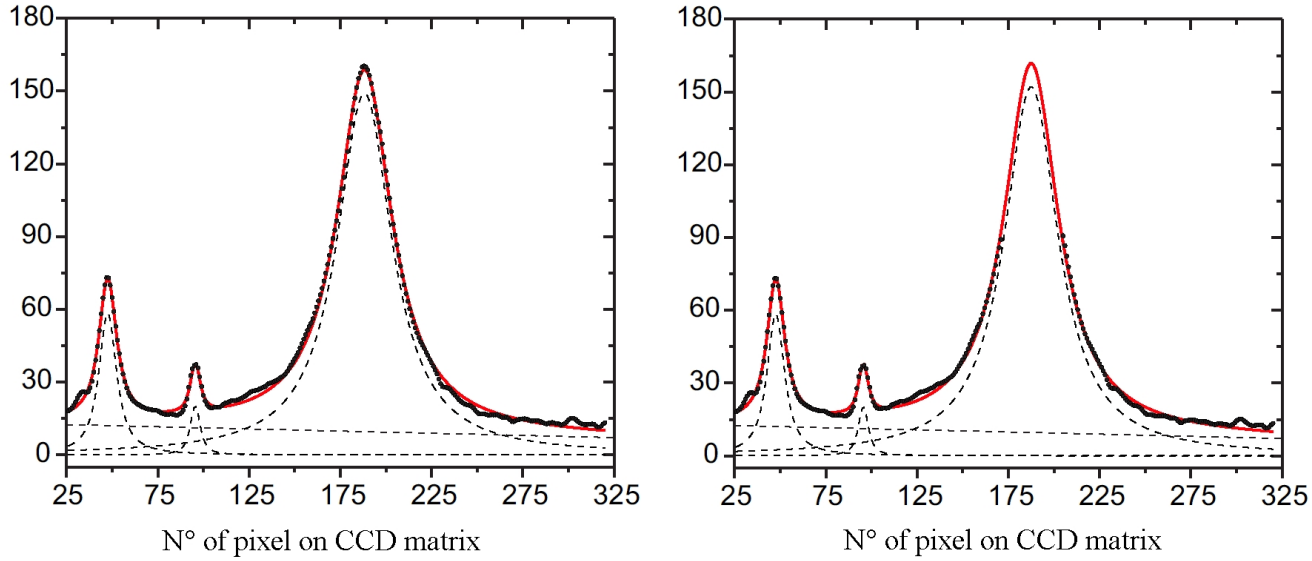

Figure 9 (Art_Wel04 Fig-09.jpg)

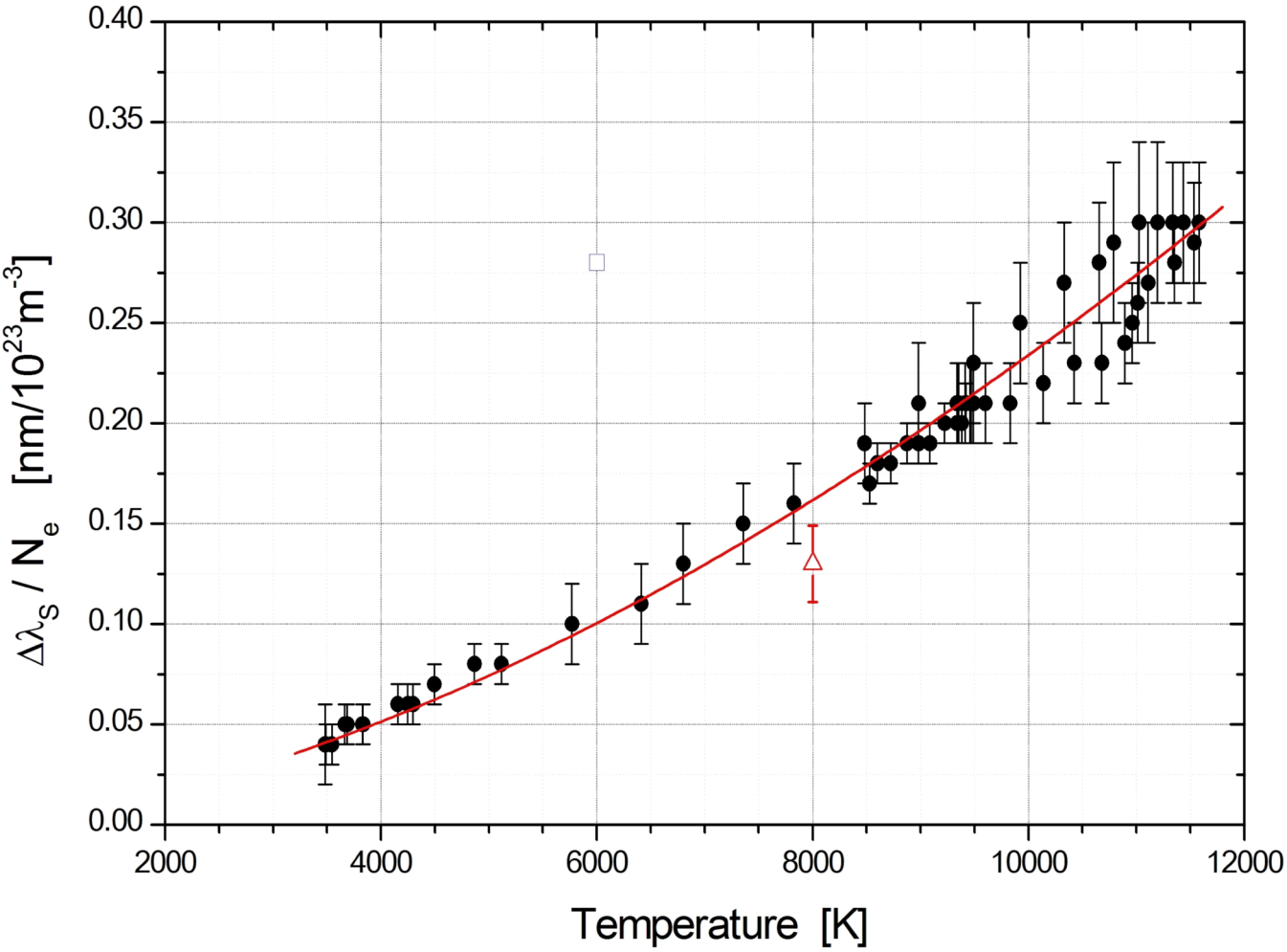

Figure 10 (Art_Wel04 Fig-10.jpg)